DOI: 10.1029/2008GL036078

Geothermal heat flux and its influence on the oceanic abyssal circulation and radiocarbon distribution

M. Hofmann[1] and M. A. Morales Maqueda[2]

Received 20 September 2008; accepted 18 December 2008; published 6 February 2009.

[1] Geothermal heating of abyssal waters is rarely regarded as a significant driver of the large-scale oceanic circulation. Numerical experiments with the Ocean General Circulation Model POTSMOM-1.0 suggest, however, that the impact of geothermal heat flux on deep ocean circulation is not negligible. Geothermal heating contributes to an overall warming of bottom waters by about 0.4°C, decreasing the stability of the water column and enhancing the formation rates of North Atlantic Deep Water and Antarctic Bottom Water by 1.5 Sv (10%) and 3 Sv (33%), respectively. Increased influx of Antarctic Bottom Water leads to a radiocarbon enrichment of Pacific Ocean waters, increasing Δ^{14}C values in the deep North Pacific from −269‰ when geothermal heating is ignored in the model, to −242‰ when geothermal heating is included. A stronger and deeper Atlantic meridional overturning cell causes warming of the North Atlantic deep western boundary current by up to 1.5°C.

Citation: Hofmann, M., and M. A. Morales Maqueda (2009), Geothermal heat flux and its influence on the oceanic abyssal circulation and radiocarbon distribution, *Geophys. Res. Lett.*, *36*, L03603, doi:10.1029/2008GL036078.

1. Introduction

[2] Geothermal heating through the seafloor adds only a very small contribution to the oceanic energy budget. The average geothermal heat flux currently entering the oceans is estimated to be between 93 and 101 mW m^{-2} (1 mW = 10^{-3} W) [*Pollack et al.*, 1993]. In comparison, sea surface turbulent and radiative heat fluxes can be hundreds to thousands of times larger [*Huang*, 1999]. Geothermal heating is also a seemingly lesser player from the point of view of the oceanic mechanical energy budget. Of the 2 TW (1 TW = 10^{12} W) of mechanical energy injected into the ocean by winds and tides, approximately 0.4 TW are directly available for turbulent mixing, that increases the available potential energy of the ocean and partly fuels the Meridional Overturning Circulation, or MOC [*Huang*, 1999; *Kuhlbrodt et al.*, 2007]. In contrast, *Huang* [1999, 2002] found that the potential energy that geothermal heating can generate is almost 10 times smaller: 0.05 TW. In spite of the small energies associated with geothermal heating, geothermal heat fluxes might have a measurable effect on the large-scale circulation and tracer distribution [*Adkins et al.*, 2005; *Huang and Jin*, 2002; *Mullarney et al.*, 2006; *Roussenov et al.*, 2004]. The reason for this is that, unlike surface heat fluxes, geothermal fluxes, however small, are unidirectional, always contributing towards increasing the buoyancy of the deep ocean. In addition, geothermal heat sources are situated at the bottom, while buoyancy losses occur at the surface, a configuration which, according to Sandström's Theorem [*Huang*, 1999], supports a closed MOC.

[3] Numerical studies with ocean circulation models of various complexities have found that oceanic geothermal heating can create bottom waters several tenths of a degree warmer than would exist in its absence, and help maintain a vigorous abyssal circulation [*Mullarney et al.*, 2006; *Huang and Jin*, 2002; *Adcroft et al.*, 2001]. It has also been argued by *Roussenov et al.* [2004] that, since oceanic concentrations of natural radiocarbon, notably in the Pacific Basin, are strongly controlled by the export rate of Antarctic Bottom Water (AABW), geothermal heating should affect the global distribution of Δ^{14}C.

[4] *Adcroft et al.* [2001] investigates the impact of geothermal heating on the simulated MOC of a global ocean general circulation model (OGCM) with realistic topography. They found a 25% increase in the amount of AABW that enters the Indo-Pacific Ocean upon application of a uniform geothermal heat flux of 50 mW m^{-2}. In their study, the deep North Pacific region experiences the most pronounced warming, with a temperature rise of up to 0.4°C.

[5] The study of *Adcroft et al.* [2001] used a spatially uniform geothermal heating source. However, geothermal heat fluxes vary considerably in space. The global compilation of geothermal heat fluxes of *Pollack et al.* [1993] shows that maximum values of up to 325 mW m^{-2} occur along the geologically young crests of the ocean ridges (Figure 1a) and that, as the oceanic crust ages away from the ridges, geothermal heat fluxes decline to a background value of about 50 mW m^{-2}. According to this data set, the global mean of the geothermal heat flux through the seabed is 101 mW m^{-2}, which is about twice the value used by *Adcroft et al.* [2001].

[6] In this article, we revisit the problem of assessing the impact that geothermal heating has on the MOC and the oceanic distribution of Δ^{14}C. We use a global ocean climate model and compare results from experiments with and without geothermal heat fluxes.

[7] The results of our study partly confirm the findings of *Adcroft et al.* [2001], but differ significantly in a number of aspects. Firstly, the circulation and temperature changes we obtain tend to be larger than theirs, which is mainly due to the larger and more realistic values of the geothermal fluxes used by us. Secondly, we find that geothermal heating causes an intensification of the Atlantic MOC by 10% accompanied by a deepening of the NADW cell by up to 500 meters, and a concomitant warming of the deep North Atlantic western

[1]Research Domain I, Potsdam Institute for Climate Impact Research, Potsdam, Germany.
[2]Proudman Oceanographic Laboratory (Natural Environment Research Council), Liverpool, UK.

0094-8276/09/2008GL036078

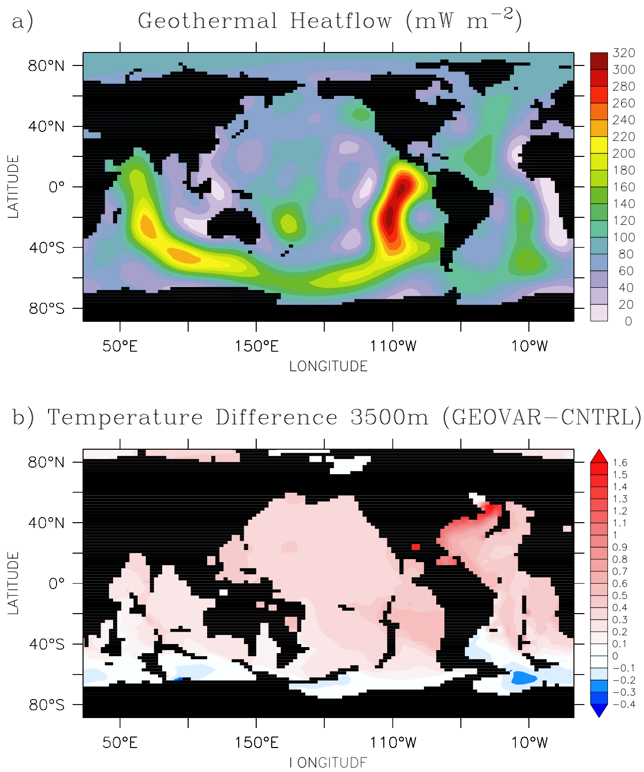

Figure 1. (a) Geothermal heat fluxes of *Pollack et al.* [1993] (in mW m^{-2}) and (b) temperature difference at 3500 m between experiments GEOVAR and CNTRL averaged over the last 200 years of integration (in °C).

boundary current by up to 1.5°C. Thirdly, a cooling of the deep Weddell Sea by up to 0.3°C is also brought about by enhanced deep ocean convection in the case when geothermal heat fluxes are applied.

2. Model and Experimental Design

[8] The model is an ocean-sea ice general circulation model coupled to an anomaly model of the atmospheric energy-moisture balance [*Hofmann and Maqueda*, 2006]. The ocean model is the Modular Ocean Model, version 3.0, featuring a number of modifications outlined by *Hofmann and Maqueda* [2006]. Henceforth, this model will be referred to as the Potsdam version of MOM, version 1.0 (POTSMOM-1.0). The horizontal model grid has a uniform resolution of 3° × 2°. In the vertical, the grid consists of 29 levels with thickness increasing from 10 m at top to 405 m at the bottom. The model includes an empirical parameterization of bottom-enhanced vertical mixing [*Hasumi and Suginohara*, 1999], with a low background diffusivity of 0.1 cm^2 s^{-1}. Isopycnic Redi stirring is set to 1.25 × 10^7 cm^2 s^{-1}, while Gent-McWilliams thickness diffusivities vary between 0.275 and 0.55 10^7 cm^2 s^{-1}. The ocean model tracers are potential temperature, salinity and radiocarbon [*Toggweiler et al.*, 1989].

[9] Three 5000-year experiments were run with this model. First, the control run (CNTRL) ignores geothermal heating. In the second run (GEOVAR), the non-uniform geothermal heat distribution of *Pollack et al.* [1993] (GEOVAR), shown in Figure 1a, was used. To test the effect of a homogeneous forcing a third experiment (GEOCONST) was conducted with a spatially uniform geothermal heat flux of 101.0 mW m^{-2}, the global average of the geothermal flux in GEOVAR. Results from the last 200 years of integration are presented here.

3. Results

[10] In accord with the results of *Adcroft et al.* [2001] and the idealized experiments of *Scott et al.* [2001], our simulations show that, on global average, geothermal heating leads to a warming of waters below the main thermocline by a few tenths of degree Celsius (0.26°C for GEOVAR and 0.22°C for GEOCONST). The newly formed, cold AABW leave the deep Antarctic Circumpolar Current (ACC), move northward and enter the Atlantic and Indo-Pacific Basins at about 40°S. As these bottom water masses flow northwards, they gradually gain heat from the geothermal sources at the sea floor. At a depth of 3500 m, the warming in the Pacific Ocean and in the eastern Atlantic Ocean simulated by GEOVAR amounts to 0.3 to 0.4 degrees (see Figure 1b). Far away from the strong geothermal sources of the mid-ocean ridges, the warming patterns calculated in experiment GEOCONST are very similar to those of GEOVAR. This is explained by the fact that geothermal warming is an integrative process: whether it occurs progressively, as a result of a uniform heat flux (GEOCONST), or discontinuously, as waters move throughout hot and cold spots (GEOVAR) is immaterial, as long as the total heat absorbed is the same in both cases.

[11] Results from GEOVAR and GEOCONST qualitatively depart from those discussed by *Adcroft et al.* [2001] in two remarkable ways. Firstly, the deep Southern Ocean, with the exception of the Amundsen and Bellingshausen Seas, experiences a cooling of up to −0.3°C. Secondly, the deep western boundary current in the North Atlantic warms by between 0.9°C and 1.5°C. Salinity changes of about −0.1 psu in the Southern Ocean and +0.1 psu in the North Atlantic accompany these temperature changes (not shown).

[12] The seemingly paradoxical cooling of the deep Southern Ocean in GEOVAR and GEOCONST is caused by an intensification of open ocean deep convection in these simulations. In all three model experiments, the occurrence of open ocean deep convection in the Southern Ocean is a prevailing feature. The main area of convection, with winter mixed layers often stretching down to the seafloor, sits astride the eastern limb of the Weddell Sea Gyre, and is centered around the Greenwich Meridian at 65°S. Smaller convection areas occur over the Cosmonaut Sea and the western Ross Sea, off Cape Adare. The convective activity in the Weddell Sea exhibits a striking inter-decadal variability. In experiment CNTRL, open deep convection occurs cyclically, with convection episodes lasting for about 20 years followed convection-free periods spanning about 30 years. The maximum area of convection is about 6 × 10^5 km^2. In both the GEOCONST and GEOVAR experiments, the area of this intermittent deep convection almost triples (Figure 2), while the period of the strong convection/weak convection cycle increases by a factor of two (not shown). We do not yet fully understand the factors

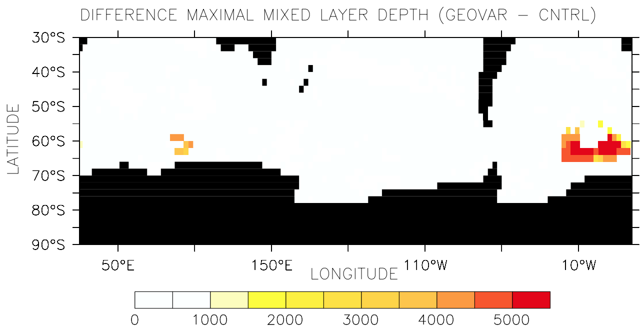

Figure 2. Difference of the maximal depth of the turbulent mixed layer over the time period of the last 200 years of simulation between GEOVAR and CNTRL in meters.

that control the frequency and intensity of the intermittent convection events, but, clearly, the more intense deep convection in GEOVAR and GEOCONST gives rise to higher rates of formation and export of AABW (Figures 3b and 3c). Convection episodes are associated with strong sea ice melt and the formation of embayments in the sea-ice cover that, in the Weddell Sea, occasionally close into a polynya, a feature also captured in the modeling study of *Goosse and Fichefet* [2001], although their polynya reappeared every winter.

[13] While the formation of recurrent polynyas in the Weddell and Cosmonaut Seas is well documented [e.g., *Moore et al.*, 2002; *Geddes and Moore*, 2007], the decadal cyclicity of the simulated polynyas and associated convection episodes is probably unrealistic. The underlying physical mechanism of these oscillations is not difficult to understand, and is as follows. In the Southern Ocean, and specially in the Weddell Sea, a sharp but weak pycnocline, well reproduced by POTSMOM-1 [*Hofmann and Maqueda*, 2006], separates the upper mixed layer from the hardly stratified ocean interior. The thermohaline structure of the water column, that is relatively fresh water close to the freezing point at the surface overlaying saltier (+0.2 psu) and warmer (+2°C) water, is such that thermobaric convection [*McPhee*, 2003] is easily triggered by minor initial instabilities caused by brines rejected during sea ice formation. Repeated deep convection over decades leads to a gradual cooling and freshening of the ocean interior. Eventually, the water column becomes too homogeneous to support thermobaric instabilities, and winter convection then ceases. The dense water thus formed is eventually flushed northward, while isopycnic eddy mixing and transport, both processes parameterized as in *Griffies* [1998], bring heat from the subtropics into the Southern Ocean, leading to a gradual re-warming of the ocean interior (Figures 2a–2c). When the thermal "rebound" of the water column is completed, a new cycle of thermobaric convection starts.

[14] The impact of geothermal heating on AABW circulation is most prominent in the Indo-Pacific Ocean. In CNTRL, the northbound flow of AABW at 30°S is 10 Sv, while in GEOVAR and GEOCONST this flow increases by about 40% thus leading to a more vigorous ventilation of the deep North Pacific compared to CNTRL (Figures 3b and 3c). This result is in qualitative agreement with *Adcroft et al.* [2001], who, with a mean geothermal heat flux equal to roughly half ours, reported an increase of 25% in deep AABW flow into the Indo-Pacific. A larger export of AABW is expected to decrease the age of North Pacific waters, and this is borne out by the fact that the deep Δ^{14}C minimum of −269‰ in CNTRL, increases in GEOVAR to −242‰ (Figures 3b and 3c), a value that compares well with recent observational data [*Key et al.*, 2004] (Figure 3a).

[15] The warming of the deep western boundary current shown in Figure 1b is the manifestation of a deepening of the North Atlantic Deep Water (NADW) overturning cell by 300 to 500 m, which also causes an increase in salinity and in Δ^{14}C (by up to 14‰ not shown). This deepening results from the increased contrast between the density of newly formed NADW and that of the AABW reaching the North Atlantic, which is as much as 0.1 kg m^{-3} lighter in GEOVAR than in CNTRL (Figure 4b). Ultimately, upwelling of this lighter water in the Southern Ocean creates a stronger meridional density contrast in GEOVAR compared to CNTRL, and a

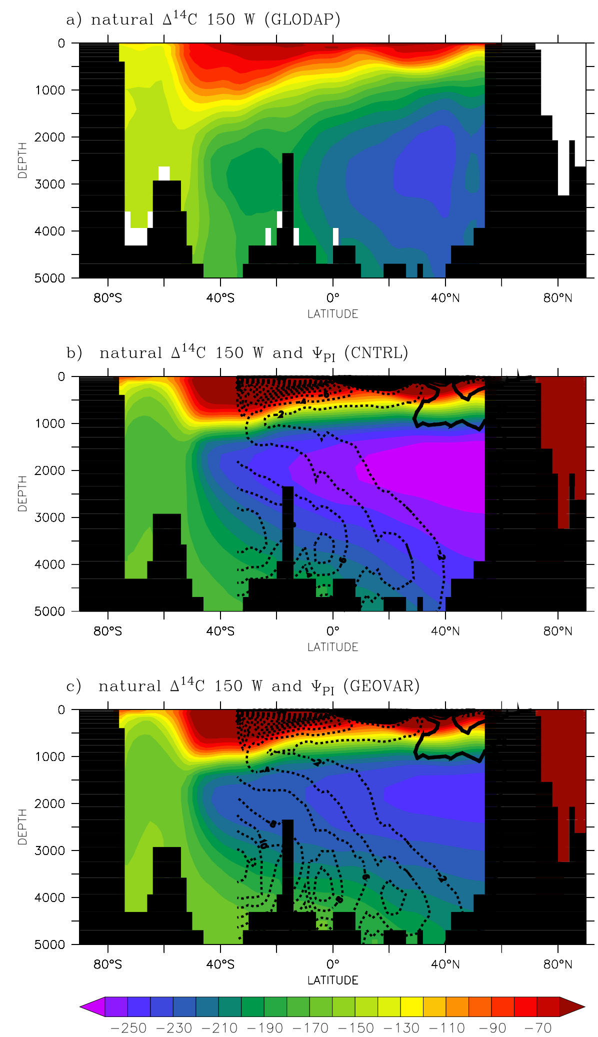

Figure 3. (a) Observed natural Δ^{14}C (in ‰) at 150° W from the Global Ocean Data Analysis Project, GLODAP [*Key et al.*, 2004]. (b) Color as in Figure 3a but simulated in CNTRL. Contours: 200-year mean of Indo-Pacific meridional overturning transport north of 34°S (in Sv) in CNTRL. The contour interval is 2 Sv. (c) As in Figure 3b but simulated in GEOVAR.

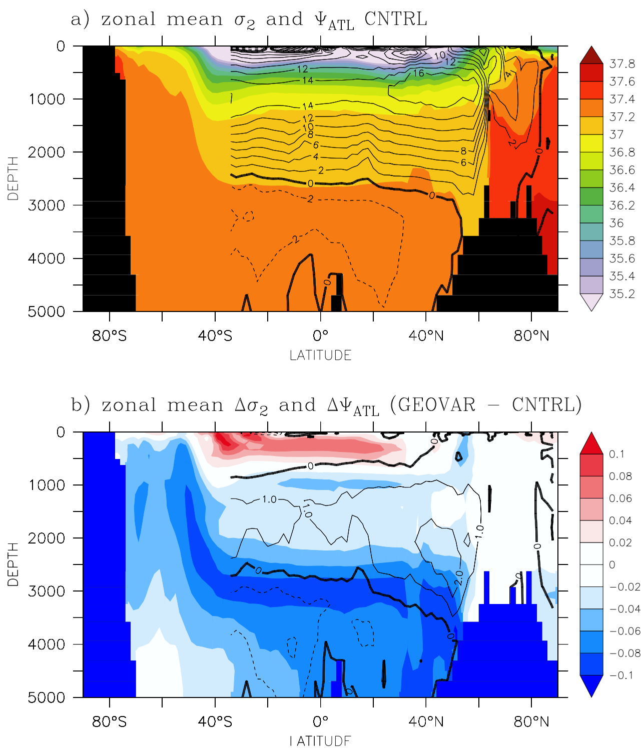

Figure 4. (a) Color fill of 200-year mean of zonally averaged σ_2 (in kg m^{-3}) and contours of 200-year mean of meridional overturning transport (in Sv) in the Atlantic Ocean north of 34°S for CNTRL. (b) As in Figure 4a, but difference between GEOVAR and CNTRL.

concomitant increase of 1.5 Sv (10%) in the strengths of the Atlantic MOC maximum and 30°S outflow.

4. Conclusions

[16] Numerical experiments with a coarse resolution ocean-sea ice model indicate that geothermal heat fluxes are a non negligible forcing of the ocean circulation, substantially strengthening the AABW and NADW overturning cells. Geothermal heating stimulates convective activity in the Southern Ocean and, consequently, increases the rate of formation and export of AABW by 33%. While the recurrent open ocean convection that produces most of the AABW in the model has rarely been observed, there is indirect evidence that sporadic thermobaric convection could indeed substantially contribute to the formation of AABW [*McPhee*, 2003]. This enhanced production of AABW leads to a better representation of the distribution of natural Δ^{14}C. In a recent study, *Matsumoto and Key* [2004] pointed out that, in ocean models with vertical diffusivities as low as observed, such as ours, the deep ocean will become less ventilated, and natural Δ^{14}C values will thus be underestimated. Here we have shown that the inclusion of geothermal heat fluxes can partly correct this pathological behavior. Geothermal heat fluxes also intensify by around 10% both the maximum of the Atlantic MOC and the outflow of NADW into the Southern Ocean, while the penetration depth of NADW in the North Atlantic is increased from 2500 m to a more realistic 3000 m.

[17] **Acknowledgments.** M. H. was funded by the Garry Comer foundation. We are grateful to E. Bauer and R. Calov for constructive comments on the manuscript.

References

Adcroft, A., J. R. Scott, and J. Marotzke (2001), Impact of geothermal heating on the global ocean circulation, *Geophys. Res. Lett.*, *28*, 1735–1738.
Adkins, J., A. P. Ingersoll, and C. Pasquero (2005), Rapid climate change and conditional instability of the glacial deep ocean from the thermobaric effect and geothermal heating, *Quat. Sci. Rev.*, *24*, 581–594.
Geddes, J. A., and G. W. K. Moore (2007), A climatology of sea ice embayments in the Cosmonaut Sea, Antarctica, *Geophys. Res. Lett.*, *34*, L02505, doi:10.1029/2006GL027910.
Goosse, H., and T. Fichefet (2001), Open-ocean convection and polynia formation in a large-scale ice-ocean model, *Tellus, Ser. A*, *53*, 94–111.
Griffies, S. M. (1998), The Gent-McWilliams skew-flux, *J. Phys. Oceanogr.*, *28*, 831–841.
Hasumi, H., and N. Suginohara (1999), Effects of locally enhanced vertical diffusivity over rough bathymetry on the world ocean circulation, *J. Geophys. Res.*, *104*, 23,367–23,374.
Hofmann, M., and M. A. M. Maqueda (2006), Performance of a second-order moments advection scheme in an ocean general circulation model, *J. Geophys. Res.*, *111*, C05006, doi:10.1029/2005JC003279.
Huang, R. X. (1999), Mixing and energetics of the oceanic thermohaline circulation, *J. Phys. Oceanogr.*, *29*, 727–746.
Huang, R. X. (2002), Corrigendum, *J. Phys. Oceanogr.*, *32*, 1593.
Huang, R. X., and X. Jin (2002), Deep circulation in the South Atlantic induced by bottom-intensified mixing over the midocean ridge, *J. Phys. Oceanogr.*, *32*, 1150–1164.
Key, R. M., A. Kozyr, C. L. Sabine, K. Lee, R. Wanninkhof, J. Bullister, R. A. Feely, F. Millero, C. Mordy, and T.-H. Peng (2004), A global ocean carbon climatology: Results from Global Data Analysis Project (GLODAP), *Global Biogeochem. Cycles*, *18*, GB4031, doi:10.1029/2004GB002247.
Kuhlbrodt, T., A. Griesel, M. Montoya, A. Levermann, M. Hofmann, and S. Rahmstorf (2007), On the driving processes of the Atlantic meridional overturning circulation, *Rev. Geophys.*, *45*, RG2001, doi:10.1029/2004RG000166.
Matsumoto, K., and R. M. Key (2004), Natural radiocarbon distribution in the deep ocean, in *Global Environmental Change in the Ocean and on Land*, edited by M. Shiyomi et al., pp. 45–58, Terrapub, Tokyo.
McPhee, M. G. (2003), Is thermobaricity a major factor in southern ocean ventilation?, *Antarct. Sci.*, *15*, 153–160.
Moore, G. W. K., K. Alverson, and I. A. Renfrew (2002), A reconstruction of the air-sea interaction associated with the Weddell Polynia, *J. Phys. Oceanogr.*, *32*, 1685–1698.
Mullarney, J. C., R. W. Griffiths, and G. O. Hughes (2006), The effect of geothermal heating on the ocean overturning circulation, *Geophys. Res. Lett.*, *33*, L02607, doi:10.1029/2005GL024956.
Pollack, H. N., S. J. Hurter, and J. R. Johnson (1993), Heat flow from the Earth's interior: Analysis of the global data set, *Rev. Geophys.*, *31*, 267–280.
Roussenov, V., R. G. Williams, M. J. Follows, and R. M. Key (2004), Role of bottom water transport and diapycnic mixing in determining the radiocarbon distribution in the Pacific, *J. Geophys. Res.*, *109*, C06015, doi:10.1029/2003JC002188.
Scott, J. R., J. Marotzke, and A. Adcroft (2001), Geothermal heating and its influence on the meridional overturning circulation, *J. Geophys. Res.*, *106*, 31,141–31,154.
Toggweiler, J., K. Dixon, and K. Bryan (1989), Simulation of radiocarbon in a coarse-resolution world ocean model: 1. Steady state prebomb distributions, *Rev. Geophys.*, *18*, 8217–8242.

M. Hofmann, Research Domain I, Potsdam Institute for Climate Impact Research, Telegrafenberg A26, D-14473 Potsdam, Germany. (hofmann@pik-potsdam.de)
M. A. Morales Maqueda, Proudman Oceanographic Laboratory, 6 Brownlow Street, Liverpool L3 5DA, UK. (mamm@pol.ac.uk)